ZIBELINE INTERNATIONAL™ PUBLISHING

ISSN: 2616-4302 (Online)
CODEN: AMMCFL

Acta Mechanica Malaysia (AMM)

DOI: http://doi.org/10.26480/amm.02.2023.72.75

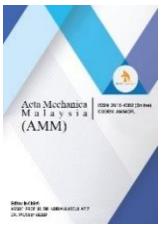

RESEARCH ARTICLE

THE STUDY ABOUT RELATIONSHIP BETWEEN CO-APERTURE SPLITTING RATIOS AND LASER FAR-FIELD SPOT MORPHOLOGY AND POWER

Shuping Miao[a], Feng Lin[b], Zhaobing Chen[b*], Yiwei Xiong[c]

[a]Sichuan Wisepride Insustry Co., LTD, Chengdu, China
[b]Changchun Institute of Optics, Fine Mechanics and Physics, Chinese Academy of Science, Changchun, China
[c]Chengdu Shuan0gliu Meteorological Service, Chengdu, China
**Corresponding Author Email: chenzhaobing2010@163.com*

ARTICLE DETAILS

Article History:

Received 25 February 2022
Revised 27 March 2023
Accepted 29 April 2023
Available online 01 June 2023

ABSTRACT

To address the problem of difficult to determine the beam splitting ratio of the spectroscopic system which results from the overlapping optical paths for laser emission and imaging in laser countermeasure shared aperture system, this paper conducts a field experiment which investigates the relationship between laser spot size control and the far-field spot morphology and the energy density magnitude at the central spot using the 3.7$\boldsymbol{\mu m}$ mid-wave infrared laser band as the light source. After setting up the field test conditions the laser pattern and energy in the far field is measured steadily by changing the stop size at the front of the laser near the conventional 86.5% laser energy. By analysis in the case of 30% to 70% laser energy outer ring blocking light, the maximum change in spot size is 1/3, the energy in the centre of the spot is affected considerably, in a non-linear relationship, especially after the blocking of light in more than 30% energy drops sharply.

KEYWORDS

Laser; power density; spot morphology; co-aperture system; laser countermeasure

1. INTRODUCTION

Co-aperture laser countermeasure systems mostly employ beam splitting to separate and combine the outgoing laser and incident tracking beams. Due to the size and weight constraints of the system, the laser beam and the imaging beam must be closely matched to achieve a reasonable beam splitting system so that the laser beam is emitted in as full a spot as possible while the imaging spot is fully recaptured（Chen et al., 2023; Guo et al., 2018).The conventional view is that 86.5% of the full laser spot is the core beam of the laser beam and this is the basis for the design of the spectroscopic system. Current laser countermeasures require increasingly smaller and lightweight systems, and the reduction of the optical size of systems has become one of the major issues requiring further research in this field. (Han et al., 2020).This paper is based on a spatial laser beam splitter scheme to conduct an experiment-based far-field laser power density calibration at a spot size near 86.5% of the spot diameter（Chen et al., 2019; Chen et al., 2018. Through the experiments found that the laser power density in the central region of the far-field spot did not change dramatically when the mid-wave infrared laser with a central wavelength of 3.7μm is below 20% of the full spot block. It can be considered that a co-aperture system in this band can control the beam splitting ratio to less than 4:1, so that the requirements of laser countermeasure systems can be met with the central spot power density of the far field as the core pursuit. For focusing systems in laser system applications, this blocking and beam splitting can seriously affect the total laser power and therefore this proportional blocking is not suitable for systems which feature non-collimated laser system applications as a central feature (Chen et al., 2017).

2. INTRODUCTION TO THE CO-APERTURE LASER SYSTEM

A co-aperture laser system is characterised by the fact that the laser emission light path and the imaging light path are physically structured as the same light path, which fulfills the goal of "pointing and hitting"(Li et al., 2018). Co-aperture systems are classified as passive co-aperture and active co-aperture (Ma et al., 2021). The laser spot splitting problem studied in this paper is mainly reflected in active beam splitting systems. This is because active beam splitting systems produce imaging echoes in the same wavelength band, which means that the emitted and imaging light are overlapping in the spectrum, and such a splitting system is very complex in design (Pan et al., 2020; Chen and Gao., 2021). The principle of optical close-loop for co-aperture based on active detection is shown in Figure 1. Active detection laser echoes are generated when the active illumination laser hits the target's optical system. The echoes are passed through a co-aperture transmitter-receiver optical unit, a fast steering mirror, a spectroscope and then detected by a high frame rate, high spatial resolution, narrow spectrum, narrow field of view imaging detector to produce an image of the target. The off-target which is the angular deviation of the angle corresponding to the precise position of the target from the line of sight of the co-aperture transmitter-receiver optical system is calculated by the image processing unit. The servo controller generates control signals based on the values of off-target and drives a fast steering mirror driven by a piezoelectric ceramic or voice coil motor to precisely correct the direction of the blinding laser emission axis in real time, allowing the laser to be aimed quickly and precisely at the incoming target optical system to achieve high precision closed-loop guidance of the incoming target. Due to the co-aperture transmitter-receiver optical design, the tracking axis is the pointing axis, and the pointing axis is the laser optical axis (line of sight), which effectively solves the problem of large jitter of the laser beam on the tracking target and improves the tracking accuracy and countermeasure effectiveness.

Active co-aperture optical closed loop beam splitting systems have high requirements in terms of the size of the beam splitter and the beam splitting area matching. The key to the design of such systems is how to effectively use the beam splitting system to increase the imaging luminous flux without reducing the energy of the laser beam (Zhang et al.,2020). The

Quick Response Code	Access this article online	
	Website: www.actamechanicamalaysia.com	**DOI:** 10.26480/amm.02.2023.72.75

Cite the Article: Shuping Miao, Feng Lin, Zhaobing Chen, Yiwei Xiong (2023). The Study About Relationship Between Co-Aperture Splitting Ratios and Laser Far-Field Spot Morphology and Power. *Acta Mechanica Malaysia, 6(2): 72-75.*

spot size of the laser beam directly determines the size of the beam splitter, so the precise design of the spot size of the laser is one of the key bases for detailed system design. The traditional empirical value of 86.5% spot size is no longer able to accurately control the quantitative design of the system in this type of system application, so a more reliable approach is to investigate the relationship between spot size and far-field laser energy for a specific wavelength laser by means of a one-to-one field experiment.

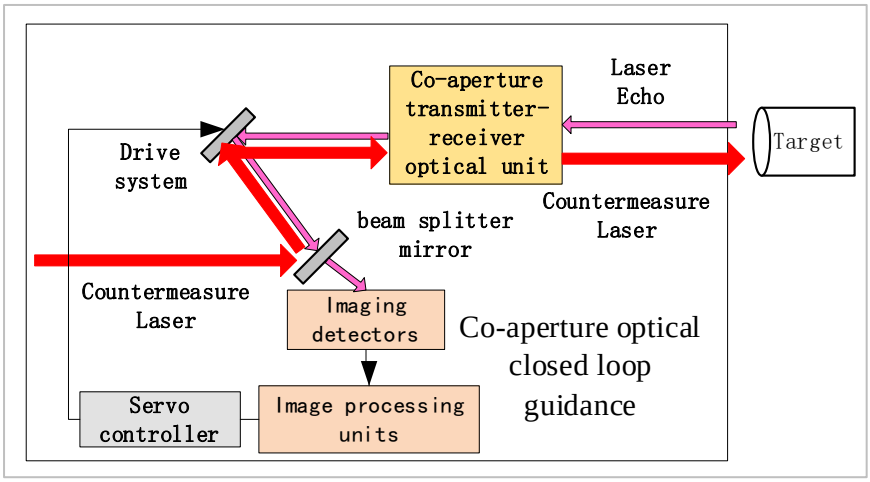

Figure 1: Principle diagram of optical closed-loop beam splitting guidance for co-aperture

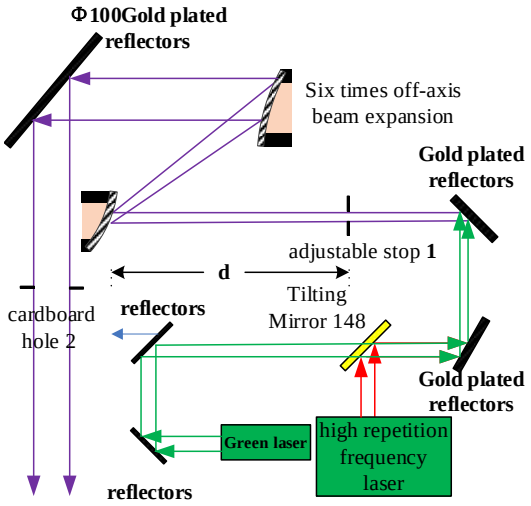

Figure 2: Schematic diagram of the optical path at the transmitter

3. Experimental Design for Laser Spot Control

This paper investigates the relationship between the spot size of a 3.7um laser beam and the spot power density at the centre of a far-field projected laser, and builds a corresponding test platform. The parameters of the laser are shown in Table 1.

Table 1: Laser Parameters

Items	**3.7μm** high repetition frequency laser
Wave length	3.71-3.73μm
Power	2.5W
Exit beam spot diameter	≤7mm
Divergence angle	5mrad
Repetition frequency	12kHz
Off-axis beam expansion factor	Six times
System exit laser divergence angle	0.8 mrad

The optical path is built according to the actual optical design structure, and the experimental optical path structure is shown in Figure 2.

After the test optical path has been set up, the original parameters of the laser emission and the far-field spot morphology, distribution and central edge power density are first measured and recorded. The laser blocking ratio at the beam splitter is then changed and the far-field spot power density is tested simultaneously, the experimental results are analysed and the corresponding conclusions are obtained. The specific test procedure is as follows.

a) At the laser exit D, the spot diameter d0 is tested using the hole-set method, requiring d0 ≈ 10 mm (98% energy) to ensure that the distance from the laser exit to the 6 times off-axis beam expanding secondary mirror is ≤ D.

b) Testing the laser power (3 levels).

c) A reflective focusing mirror with focal length f=3m is used to test the laser's original divergence angle θ_0 (without stop).

d) The laser spot shape (diagram), spot size, and energy distribution (measured at 5 points on a unit scale of "half the distance from the centre of the spot to the edge", top, bottom, left, right and centre) are tested at approximately 120m.

Build the optical path of the emitter according to Figure 2, described in the following procedure.

a) Optical alignment of Beam Combiner (Tilting Mirror 148)

After the laser has passed through the beam combiner, test the power (above 95%) and then observe the spot shape at 120m. If at this point the spot shape matches the original spot shape of the laser, the commissioning continues.

b) Alignment for laser coupling

Combining green light with a laser beam.

c) Commissioning of gold-plated reflectors and beam expansion systems

The two gold-plated mirrors are commissioned so that the centre of the green light hits the centre of both the secondary beam expander and the primary mirror. After the laser has passed through the beam expanding system, the spot shape is observed with the camera at 120m. If the spot shape is the same as the original spot shape of the laser at this point, the commissioning continues.

The process of building the target is as follows: the distance L between the laser transmitter and the laser receiver plate is about 400m, and the distance D1 between the medium wave camera and the laser receiver plate is about 10m, so that the laser receiver plate is fully imaged in the camera. Adjust the angle and pitch of the Φ100 gold-plated reflector to make the green light hit the target. With the green light turned off and the laser out at full power (Third class), the position of the medium wave laser is observed with the medium wave camera so that all of the medium wave laser is received by the target.

An adjustable stop is added in front of the beam expanding system and the distance L1 between the stop and the 6 times off-axis beam expanding secondary mirror is recorded. Adjustable stop aperture centre alignment to the laser spot centre. After adjustment of the adjustable stop clear aperture to make the laser emission at 30% / 40% / 50% / 60% / 70% / 80% / 86.5% / 90% / 100% of the full power (before and after the stop), the aperture diameter d1 is recorded. Add cardboard hole 2 after the beam expanding system and record the distance L2 between the cardboard hole and the Φ100 gold plated reflector. The centre of the cardboard hole is aligned with the centre of the laser spot and the laser power (reflected focus) is tested by changing different cardboard holes (apertures d2 are 20mm, 30mm, 40mm, 50mm, 60mm, 70mm).

4. Experimental Data Gathering

Without the cardboard hole 2, the adjustable stop diameter d1 (the value recorded in the previous experiments) is adjusted and the laser emits at the 2nd and 3rd power levels respectively. The spot shape is observed using a medium wave camera and recorded by taking screenshots or taking photographs and then measuring the spot diameter directly with a straight edge. The adjustable stop is fully open and the laser emits at 2nd and 3rd power levels respectively by changing different cardboard holes 2 (apertures d2 are 20mm, 30mm, 40mm, 50mm, 60mm, 70mm). The spot size is then recorded by using the medium wave camera. The energy box and its ancillary facilities are positioned that the centre of the laser spot coincides with the centre of the energy box. Without the cardboard hole 2, the adjustable stop's clear aperture d1 is adjusted (to the value recorded in the previous experiment) and the laser power is tested using the energy box and power meter. Add cardboard holes of 40mm and 60mm in front of the energy box1 and test again. Adjustable stop fully open, change different cardboard holes 2 (holes d2 of 20mm, 30mm, 40mm, 50mm, 60mm, 70mm) and test laser power using energy box and power meter. Cardboard holes of 40mm and 60mm diameter are added in front of the energy box1 and tests are carried out again. Using the "half distance from the centre of the spot to the edge" as the unit scale, the energy box and its ancillary facilities are positioned and the laser power is tested at four points, top, bottom, left and right, according to the previous procedure.

In this study, the power of the laser is measured in 2nd class, the diaphragm diameter is adjusted to ensure stable light source jitter and the test error is controlled, and the power density at the far-field laser shape and central spot is recorded. Table 2 shows the far-field spot shapes for different stop diameters.

Table 2: Far-Field Spot Morphology Under Different Laser Stop Conditions

Adjustable stop luminous diameter d1 (mm)	Laser power	2nd power laser spot diameter（mm）	
		direction of the top and bottom	direction of the left and right
1.45	30%	207	236
1.89	40%	216	220
2.1	50%	210	224
2.39	60%	205	213
2.42	70%	206	210
3.23	80%	245	215
3.62	86.5%	250	250
4.34	90%	270	244
Full open	100%	304	264

Table 3: Far-Field Laser Power Tests

Adjustable stop luminous diameter d1 (mm)	Laser power	Power (mW) at cardboard hole 1 (40 mm)			Power (mW) at cardboard hole 1 (60 mm)			Power (mW) without cardboard hole		
1.45	30%		4.1			10			25	
		2.81	13	3.6	5.8	25	7.6	13	70	17
			4.5			10			24	
1.89	40%		4.7			11			32	
		8.1	24	7.1	17	54	15	41	130	37
			40			86			190	
2.1	50%		6.2			14			46	
		11	24	7.6	27	53	16	63	130	40
			53			115			247	
2.39	60%		6.9			17			50	
		13	37	14	38	72	33	87	177	80
			80			174			368	
2.42	70%		7.1			19			52	
		13	33	24	45	82	46	105	185	133
			72			155			333	
3.23	80%		16			37			101	
		21	58	30	60	125	66	144	340	210
			120			256			525	
3.62	86.5%		22			54			152	
		24	57	51	68	130	128	173	325	310
			133			282			570	
4.34	90%		37			86			231	
		42	93	70	99	200	145	230	430	390
			122			275			550	
Full open	100%		40			97			255	
		37	94	81	86	185	170	210	420	420
			103			240			500	

The results of the far-field power tests are shown in Table 3.

5. Analysis of The Effect of Stop Blocking on Far-Field Spot Size and Central Power

Analysis of the above resultant experimental test results leads to a trend in laser spot size as shown in Figures 3 and 4.

Figure 5 shows the results of an experimental analysis of the energy at the centre of the far-field laser spot.

From the results of the above analysis, it can be seen that the blocking laser has an effect on the spot size, morphology and central laser energy in the far field. In the field of laser countermeasure the variation of the spot size is not important and the spot size in the maximum blocking condition (minimum laser power emitted) is 2/3 of that in the left and right directions and does not vary significantly in the upper and lower directions. It can be assumed, therefore, that the blocking of light has little effect on the size and shape of the laser far-field spot. The far-field energy diagram shows that the laser centre energy becomes smaller after blocking, especially below 70% laser power, the far-field laser centre spot energy drops sharply.

6. Conclusion

This paper investigates the splitting ratio of the key beam splitter part of the co-aperture system and performs an external field test for verification of the mid-wave laser blocking ratio based on the variation of the laser far-field spot morphology size and the central spot energy magnitude. From the results the effect of light blocking on the far-field spot size is negligible in laser countermeasure applications. The different blocking ratios have a non-linear effect on the far-field spot centre energy. It is important to avoid blocking the light as much as possible when conditions allow, so that the central energy of the far-field spot is guaranteed. If the system design is challenging, the blocking ratio of the laser beam must not be greater than 30%, otherwise the energy drop in the far-field centre spot will be very drastic.

References

Chen Z-B, Chen N, Shi K, Li, G., 2018. The Research about High Dynamic and Lowgray Target Image Differential Capture Technology Based on Laser Active Detection. EURASIP Journal on Image and Video Processing, 1.

Chen Z-B, et al., 2023. The research about application of quasi-zero stiffness vibration isolation technology in a large vehicle-mounted optic-electronic equipment. Ain Shams Engineering Journal, 14, Pp. 101841-101851.

Chen Z-B, Li G-N, Liu X-Y, Liu, X-Y., 2017.The structure form layout and installation design about car-based photonics mast. Discrete Mathematical Sciences Cryptography, 20, Pp.231–238.

Chen, X., Gao, M., 2021. Design of Airborne Dual-Band Common Aperture Photoelectric Aiming Optical System. Infrared and Laser Engineering, 50(5), Pp. 155.

Chen, Z-B., Shi,K., Chen, N., Shi, L., 2019. The experimental study about laser-induced dizziness effect of medium-wave infrared seeker which based on image processing. J Vis Commun Image R, Pp. 59.

Guo Yulin, Yu Xun, Cai Kejun, et al., 2018.Optical Design of TV/IR Dual-Band Common -Aperture System. Infrared Technology, 40(2), Pp. 125.

Han Peixian, Ren Ge, Liu Yong, Guo Junli, Zhou Jianwei , Cui Zhangang., 2020.Optical Design of VIS/MWIR Duai-Band Common-Aperture System. Journal of Applied Optics, 41(3),Pp. 435.

Li J,Cha Y, Wang J ,Jiaan, W., Sun, M.K., Shuang, L., 2018.Optical system design for multi-special laser radar with refraction and reflection in co-path. Chinese Journal of Lasers, 45(5), Pp. 267-272.

Ma Zhanpeng, Wang,H., Shen, Y., Wang, F., Xue, Y., 2021. Design and Realization of Visible/LWIR Dual-Color Common Aperture Optical System. Acta Photonica Sinica, 50(5), Pp. 32.

Pan Lu, Xiang Yang, Li Qi, et al., 2020.Design of Visible Light and Long Wave Infrared Duai-Band Common Aperture Optical System. Journal of Changchun University of Science and Technology, 43(6),Pp. 1.

Zhang H W, Ding Y L, Ma Y J, et al., 2020.Design of infrared Dual-Band/Dual-FOV imaging early waring system. Optics and Precision Engineering, 28(6),Pp. 1283-1294.